Journal of Building Engineering 112 (2025) 113774

Contents lists available at ScienceDirect

Journal of Building Engineering

journal homepage: www.elsevier.com/locate/jobe

Adaptive neural temporal hybridization for missing data imputation in building energy use datasets: An integrated LNN-LSTM weighted model

Saeed Murtaza [a], Sarath Raj [a], Geun Young Yun [a,*], Duk-Joon Park [b], Ji-Hye Kim [b], Gwanyong Park [b], Jin Woo Moon [c]

[a] Department of Architectural Engineering, Kyung Hee University, 1732, Deogyeong-daero, Giheung-gu, Yongin-si, Gyeonggi-do, 17104, Republic of Korea
[b] Zero Energy Building Center, Korea Conformity Laboratories, Seoul, 06711, Republic of Korea
[c] School of Architecture and Building Science, Chung-Ang University, 84 Heukseok-ro, Dongjak-gu, Seoul, Republic of Korea

ARTICLE INFO

Keywords:
Adaptive neural networks
Building energy
Liquid neural network
Long short-term memory
Integrated weighted model

ABSTRACT

Accurate and complete building energy consumption data is essential for optimizing energy efficiency, forecasting demand, and supporting energy management systems. However, missing data from sensor malfunctions or communication failures can reduce the effectiveness of data-driven decision-making. This study introduces the integrated LNN-LSTM weighted model (ILLWM), a novel imputation approach that combines the adaptability of liquid neural networks (LNN) with the temporal modeling capabilities of long short-term memory (LSTM) models. Imputed values are generated using an RMSE-based weighted approach. ILLWM was tested on real-time energy consumption data from three building types, missing completely at random scenarios with missing rates of 20 %, 30 %, and 40 %. Results showed ILLWM significantly outperformed other imputation methods, including Soft-Impute, KNN, RF, SVM, MLP, Transformer networks, LSTM, and LNN. For commercial buildings with 40 % missing data, ILLWM achieved RMSE reductions of 76.9 % and 89.6 % over LNN and LSTM, respectively. For hospital buildings, improvements included RMSE reductions of 6.12 % over LNN and 31.93 % over LSTM. The ILLWM closely matched actual data, outperforming traditional and machine learning approaches. These results demonstrate the potential of the ILLWM to enhance data reliability, enabling more accurate energy demand forecasting and the development of sustainable energy management strategies in diverse building environments.

1. Introduction

Global energy demand continues to rise, driven by population growth, urbanization, and increased energy consumption across various sectors, with buildings accounting for about one third of total energy use worldwide [1]. The growing energy demand, coupled with the urgent need to mitigate climate change, has led to the widespread adoption of Building Energy Management Systems (BEMS) to improve energy efficiency, optimize consumption, and reduce environmental impact [1]. Enhanced by advancements in machine

* Corresponding author.
E-mail address: gyyun@khu.ac.kr (G.Y. Yun).

https://doi.org/10.1016/j.jobe.2025.113774
Received 14 May 2025; Received in revised form 17 July 2025; Accepted 12 August 2025
Available online 14 August 2025

Nomenclature

ILLWM	Integrated LNN-LSTM Weighted Model
LNN	Liquid Neural Network
LSTM	Long Short-Term Memory
ML	Machine Learning
MLP	Multilayer Perceptron
RF	Random Forest
SVM	Support Vector Machine
ODE	Ordinary Differential Equation
MCAR	Missing Completely at Random
RMSE	Root Mean Square Error
AMI	Advanced Metering Infrastructure
KEPCO	Korea Electric Power Corporation
KNN	k-Nearest Neighbors
PI-DAE	Physics-Informed Denoising Autoencoder
CNN	Convolutional Neural Network
RNN	Recurrent Neural Network
GAN	Generative Adversarial Network
NAS	Neural Architecture Search

learning (ML) and artificial intelligence (AI), BEMS is transforming the energy sector by addressing complex analytical challenges and enabling more efficient energy management [2]. A key component of its efficiency is accurate electric load forecasting, which heavily depends on large amounts of automated metering data that monitor power usage by different devices [3]. However, such data is often incomplete due to gaps arising from equipment non-functionality, signal transmission failures and physical disturbances [4,5]. Missing data has significant impact on the performance of ML algorithms, as these models rely on complete datasets for effective training. To address this issue, imputation methods are employed, which involve replacing missing values with plausible estimates while maintaining the integrity of datasets used in statistical analysis [6].

Data imputation has become increasingly important, with applications in fields such as pharmacometrics, PV generation forecasting, and energy management systems [7–9]. There are over 150 known imputation methods, generally classified into three categories: traditional statistical methods, ML approaches, and deep learning techniques [10]. Traditional methods, such as hot deck, cold deck, and mean imputation, along with advanced techniques like linear interpolation and ARIMA, often struggle to capture complex temporal patterns in real-world data [11–14]. ML-based methods, including SoftImpute, KNN, and MICE-LightGBM, improve accuracy by leveraging data relationships, while models like Random Forest (RF), Support Vector Machine (SVM), and Multilayer Perceptron (MLP) effectively handle non-linear and dynamic data [15–21]. Recently, deep learning architectures such as generative adversarial networks (GANs), recurrent neural networks (RNNs), convolutional neural networks (CNNs), and self-attention mechanisms have emerged as powerful tools for imputation [22,23]. GANs excel at generating realistic data, RNNs capture temporal dependencies, CNNs identify spatial patterns, and self-attention mechanisms effectively model long-range dependencies, making them highly effective for complex data scenarios.

Data imputation has found applications in the building energy management research. Early approaches to data imputation in the building sector primarily relied on simple statistical techniques, such as mean substitution and linear interpolation. While computationally efficient, these methods often failed to capture complex dependencies in energy datasets [24]. These limitations are addressed by introducing a pattern-recognition-based ensemble framework for sensor data imputation [25]. The framework involved generating a validation dataset from sensor patterns and testing a pool of imputation methods to identify optimal approaches for each sensor. Applied to 18 sensors in a real campus building, this method demonstrated an average accuracy improvement of 18.2 % over single-method approaches, showcasing the value of customized ensemble techniques.

ML techniques have further advanced the field by leveraging building-specific characteristics to improve imputation accuracy. One study proposed a novel method based on Mixture Factor Analysis (MFA) tailored to building electric load data [26]. By incorporating insights into the variability and characteristics of building loads, this method effectively captured unique patterns, resulting in enhanced imputation performance. Findings from this study with real datasets demonstrate that MFA outperforms conventional imputation techniques, underscoring the value of incorporating domain-specific insights into data-driven energy management strategies.

Deep learning has brought transformative capabilities to data imputation by enabling the modeling of complex patterns and long-term dependencies. The LSTM-BIT (Bi-directional Imputation and Transfer Learning) model was developed by combining the sequential modeling strengths of Long Short-Term Memory (LSTM) networks with the adaptability of transfer learning [27]. This hybrid approach addressed various missing-data scenarios, including random, continuous, and high-rate missing data, and outperformed traditional methods by achieving 4.24–47.15 % lower Root Mean Error RMSE in a case study on campus laboratory energy consumption.

Another study introduced a multidimensional context autoencoder using image-based reconstruction techniques to address missing

data in building energy datasets [28]. By reshaping energy data into two-dimensional formats, the model identified spatial and temporal patterns, enhancing the accuracy of imputation for large data gaps. The study tested the Partial Convolution (PConv) method on a benchmark dataset of 1479 global energy meters, encompassing diverse building and meter types. Results demonstrated that PConv outperformed other approaches, including 1D-CNN and weekly persistence methods, by reducing Mean Squared Error (MSE) by 20 %–30 %. This research underscores the utility of deep learning techniques, such as PConv, in handling complex missing patterns and provides a scalable framework for accurate energy data reconstruction.

Deep networks also pose challenges, particularly overfitting when applied to small or sparse datasets. This issue was explored in the context of deep RNNs for energy forecasting [29]. The study tested four imputation methodologies, emphasizing the sensitivity of gap size and data availability on imputation accuracy. Regularization techniques were employed to mitigate overfitting, achieving a mean absolute error of 2.1 in forecasting tasks. This work highlighted the importance of balancing model complexity and generalizability to ensure robust performance.

Hybrid models integrating multiple architectures have demonstrated substantial advancements in imputation accuracy [30]. By incorporating a data augmentation strategy, existing deep learning models can be further optimized for reconstructing missing energy time-series, even in limited data regimes. For instance, a convolutional denoising autoencoder, combined with augmentation techniques, achieved a 37 %–48 % reduction in average RMSE for continuous and random missing data scenarios. Such strategies showcase how hybrid frameworks, like CNN-RNN models and augmentation-enhanced autoencoders, effectively address spatial and temporal inconsistencies while minimizing computational overhead, underscoring their practicality for energy data imputation. Similarly, the LSTM-BIT model exemplifies the power of hybrid approaches in overcoming the limitations of standalone techniques [27].

Recent studies emphasize the importance of interpretability and validation in building energy modeling for missing data imputation. Integrating prior knowledge, such as building physics principles, into ML frameworks improves both accuracy and practical utility. For instance, Physics-informed Denoising Autoencoders (PI-DAEs) incorporate physics-based constraints in their loss functions, enhancing interpretability while aligning with real-world energy dynamics [31]. A recent study also employed Bayesian networks to detect and rectify sensor faults in their imputation model, improving system reliability [32]. Additionally, attention mechanisms and advanced architecture have proven effective in recovering complex patterns from multivariate time-series data, particularly in scenarios with extensive missing values [33].

While a diverse array of imputation methods has emerged, which can be broadly categorized into traditional statistical methods, machine learning approaches, and deep learning techniques, it is important to acknowledge that significant challenges still persist. Traditional statistical methods such as hot deck, cold deck, mean imputation, linear interpolation, and ARIMA struggle to capture complex temporal patterns in real-world datasets, particularly when facing higher missing rates [11–14]. ML-based methods, including SoftImpute, KNN, MICE-LightGBM, RF, SVM, and MLP, have improved accuracy by leveraging data relationships, yet often falter in dynamic and high-missing-rate scenarios, especially in complex building energy datasets [15–21]. Recent advances in deep learning, such as GANs, RNNs, CNNs, and self-attention mechanisms, have shown promise due to their capacity to model temporal dependencies and complex patterns effectively [22,23]. Nevertheless, these models still face inherent limitations, including challenges in generalization, computational overhead, and performance degradation when data distributions change or become increasingly sparse [34, 35].

Recent advancements have led to the development of Liquid neural networks (LNN), based on the principles of liquid time-constant networks (LTCNs). Unlike conventional neural networks, LNNs incorporate continuous-time dynamics, enabling them to adapt more readily to dynamic, evolving data [36]. LNN's unique architecture shows promising potential for managing the complex, real-world variability of energy consumption data [37–39]. Inspired by biological systems, LNN operates as continuous-time neural networks with inherent adaptability, making them particularly effective for time-series and dynamic data [40–42]. Unlike traditional neural networks, which often struggle with noisy and variable datasets, LNN uses ordinary differential equations (ODEs) to capture complex temporal dependencies, allowing them to process real-time data more effectively [39].

LNN has found applications in various fields. For instance, in financial forecasting, LNN have outperformed traditional models by dynamically adjusting to market fluctuations, offering enhanced predictive accuracy under non-linear conditions [43]. Similarly, in communication systems, LNN have been successfully deployed to manage channel state information (CSI) in Multiple input, Multiple output (MIMO) systems, providing higher spectral efficiency and reduced computational complexity [44]. Their implementation on neuromorphic hardware for tasks like image classification has also demonstrated superior energy efficiency and accuracy [45].

A critical evaluation of recent literature identifies the following key research gaps: (i) existing methods frequently neglect high rates of missing data (20 % or more), which are common in real-world energy datasets; (ii) current imputation techniques inadequately address complex, dynamic, non-linear temporal dependencies typical of energy consumption in commercial, residential, and hospital buildings; and (iii) limited robustness and adaptability of methods under changing data conditions, particularly in Missing Completely At Random (MCAR) scenarios. To address these gaps, we propose the hypothesis that integrating LNN, known for their adaptability, with LSTM models, recognized for their temporal modeling capabilities, will substantially improve imputation accuracy. Consequently, our research addresses the question: "Can an integrated LNN-LSTM weighted model (ILLWM), leveraging LNN's adaptability and LSTM's temporal modeling, significantly outperform existing methods in accurately reconstructing missing energy consumption data in buildings under high MCAR scenarios?"

To address the limitations of current imputation methods and explore the potential of LNNs for this purpose, this study aims to:

- Introduce a novel ILLWM that effectively combines the adaptability of LNN and the robust temporal modeling capabilities of LSTM through an RMSE-based weighting mechanism.

- Conduct a comprehensive evaluation of the proposed model using real-world building energy consumption datasets across commercial, residential, and hospital buildings under varying MCAR missing rates (20 %, 30 %, and 40 %).
- Demonstrate significant improvements in imputation accuracy (lower RMSE values and higher correlation) compared to both traditional statistical methods and advanced ML-based approaches, highlighting the practical benefits of the ILLWM for enhancing data-driven decision-making in energy management systems.

The structure of this paper is organized as follows: Section 2 presents the methodology, including the proposed framework, theoretical foundations of LNN and LSTM, details on the proposed ILLWM, data collection, preprocessing, missing data introduction, benchmark models, model setup, and evaluation. Section 3 presents results, analyzing model performance using RMSE and correlation metrics. Section 4 discusses findings, ILLWM implications, and limitations. Section 5 concludes with key insights and future research directions.

2. Methodology

The methodology of this study consists of two key components: (i) the design and formulation of the proposed imputation framework (ILLWM), and (ii) the experimental process to evaluate its performance using real-world building energy datasets. The proposed framework, detailed in Section 2.1, describes the architectural design of the ILLWM, explaining the theoretical foundations of LNN and LSTM and the RMSE-based weighting mechanism. Section 2.2 onward outlines the step-by-step experimental process, including data collection, preprocessing, missing data generation, benchmark model setup, and model training and evaluation procedures. Fig. 1 presents the overall flowchart summarizing the full methodology. The process begins with data collection and preprocessing of real-world energy consumption data, followed by the artificial introduction of missing values to simulate real-world incomplete datasets. Various benchmark models, spanning traditional statistical methods and advanced machine learning techniques, are applied to establish baseline performance. Subsequently, the ILLWM is implemented by independently training the LNN and LSTM models and integrating their predictions using an RMSE-based weighting mechanism. Finally, the performance of all models is evaluated using RMSE and Pearson correlation coefficient metrics to assess the accuracy and robustness of the imputation process.

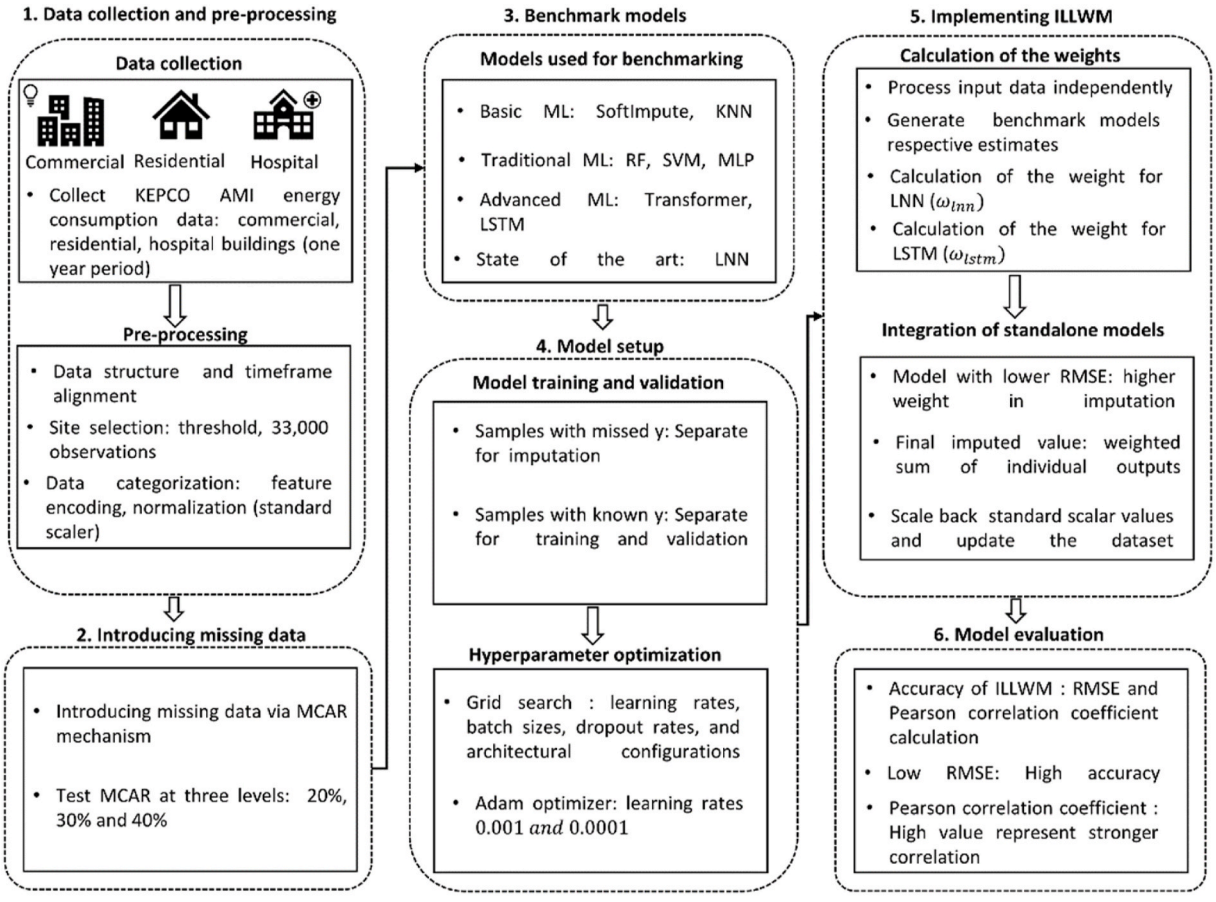

Fig. 1. Flowchart of the methodology for the ILLWM imputation process.

2.1. Proposed framework

Fig. 2 shows the architecture of the proposed ILLWM model. The process starts with preprocessed and encoded data, which is fed into the LNN and LSTM modules. The foundation for LNN and LSTM originates from RNNs, which model sequential dependencies using hidden states [51]. The outputs from these models are combined using a weighting system with fixed weights derived from RMSE calculations, integrating LNN's adaptability with LSTM's sequential modeling for an optimized imputed sequence. The subsequent sections outline the theoretical aspects of LNN, LSTM, and ILLWM. As illustrated in Fig. 2, LNN and LSTM operate independently to preserve their distinct modeling capabilities. Their final outputs are then combined through a weighted sum, with the weighting mechanism based on each model's RMSE performance on the specific dataset. The detailed explanation of this integration process is provided in Section 2.1.3.

2.1.1. LNN

LNNs advance traditional RNNs through continuous-time neural processing, enabling adaptive memory retention based on real-time variations [37]. Unlike conventional RNNs, which update hidden states at fixed time steps, LNNs employ Neural ODEs to model hidden states dynamically, as given by equation (2), [42].

$$\frac{dh(t)}{dt} = -\frac{1}{\tau(x(t))}h(t) + \text{LeakyReLU}(W_h h(t) + W_x x(t) + b) \tag{1}$$

where $h(t)$ is the hidden state at time t, $x(t)$, $\tau(x(t))$, represents a time-dependent decay factor, regulating memory retention , W_h and W_x are trainable weight matrices, and b is the bias term. The LeakyReLU is the activation function, defined as:

$$\text{LeakyReLU}(x) = \begin{cases} x, x \geq 0 \\ \alpha x, x < 0 \end{cases} \tag{2}$$

This prevents neuron saturation and ensures stable gradient propagation, with α typically set to 0.01 to ensure continuous gradient flow [46]. This choice enhances the stability of Neural ODE solvers, making LNNs particularly suitable for time-series imputation tasks.

A key feature of LNNs is their Liquid Time-Constant (LTC) mechanism, which dynamically adjusts time constants based on input characteristics. The mechanism is defined by the equation:

$$\tau(x(t)) = \tau_0 + \sum_i \alpha_i \cdot \text{LeakyReLU}(W_\tau x_i(t) + b_\tau) \tag{3}$$

where τ_0 is the base time constant , α_i is learnable scaling coefficient, and W_τ and b_τ are the trainable weight matrix and bias term, respectively. The dynamic adjustment ensures short-term adaptability while preserving longer patterns. The memory retention dynamics follow an exponential decay model:

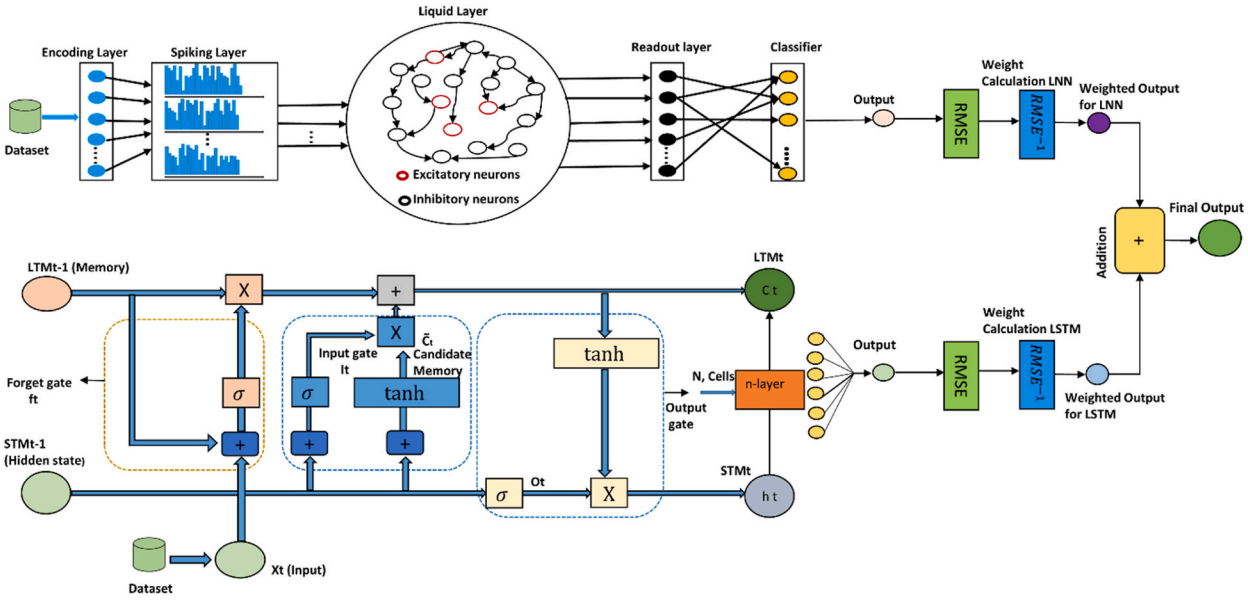

Fig. 2. Architecture model showing the integration of LNN and LSTM for imputation, including a weighting system to generate the final result.

$$h(t) = h_0 e^{-\int_0^t \frac{1}{\tau(x(\tau))} d\tau} + \int_0^t e^{-\int_\tau^t \frac{1}{\tau(x(s))} ds} \text{LeakyReLU}(W_h h(\tau) + W_x x(\tau) + b) d \tag{4}$$

The first term, $h_0 e^{-\int_0^t \frac{1}{\tau(x(\tau))} d\tau}$, represents exponential decay, controlling how past information fades over time, while the second term accumulates new information, refining the model's understanding of sequential dependencies [37,42].

2.1.2. LSTM

LSTMs employ gated recurrent units that regulate information flow across sequential time steps [47,48]. The LSTMs consists of three primary gates: the forget gate (f_t), which determines what past information to discard; the input gate (i_t), which regulates new information storage; and the output gate (o_t), which controls the contribution of stored memory to the output [47,48]. The mathematical formulation of these gates is:

$$f_t = \sigma\left(W_f[h_{t-1}, x_t] + b_f\right) \tag{5}$$

$$i_t = \sigma(W_i[h_{t-1}, x_t] + b_i) \tag{6}$$

$$o_t = \sigma(W_o[h_{t-1}, x_t] + b_o) \tag{7}$$

where h_{t-1} represents the previous hidden state, x_t is the current input, σ is the sigmoid activation function and W_f, W_i, W_o and b_f, b_i, b_o are trainable weights and biases, respectively. The cell state C_t is updated as:

$$C_t = f_t \cdot C_{t-1} + i_t \cdot \tanh(W_c[h_{t-1}, x_t] + b_c) \tag{8}$$

And the hidden state h_t is determined by:

$$h_t = o_t \cdot \tanh(C_t) \tag{9}$$

These mechanisms ensure effective long-term sequence modeling, making LSTMs particularly well-suited for energy forecasting applications [49].

2.1.3. ILLWM

The ILLWM is formulated to enhance the imputation of missing values in time-series energy consumption datasets through a systematic weighting mechanism. The transition from LNN and LSTM predictions to their weighted integration follows a structured mathematical approach to determine each model's relative contribution. Let x_i represent the input at time t containing missing values. The imputed estimates from the LNN and LSTM components are denoted as follows:

$$\widehat{y_i}, lnn = f_{LNN}(x_i) \tag{10}$$

$$\widehat{y_i}, lstm = f_{LSTM}(x_i) \tag{11}$$

where f_{LNN} and f_{LSTM} denote the imputation functions of the respective models. To quantify the imputation accuracy of each model, the RMSE is computed using the observed values in the dataset. The RMSE values for the LNN and LSTM models are given by:

$$RMSE(lnn) = \sqrt{\frac{1}{n}\sum_{i=1}^{n}(y_i - \widehat{y_i}, lnn)^2} \tag{12}$$

$$RMSE(lstm) = \sqrt{\frac{1}{n}\sum_{i=1}^{n}(y_i - \widehat{y_i}, lstm)^2} \tag{13}$$

where y_i represents the actual observed value, and n is the total number of missing values considered in the evaluation.

To optimize the imputation process, ILLWM assigns weights based on inverse RMSE values, ensuring that the model with the lower RMSE has a greater contribution to the final imputed value. The weight calculations are given by:

$$\omega_{lnn} = \frac{\frac{1}{RMSE_{lnn}}}{\frac{1}{RMSE_{lnn}} + \frac{1}{RMSE_{lstm}}} \tag{14}$$

$$\omega_{lstm} = \frac{\frac{1}{RMSE_{lstm}}}{\frac{1}{RMSE_{lnn}} + \frac{1}{RMSE_{lstm}}} \tag{15}$$

After computing the weights for each model, the final imputed value for each missing data point is obtained as a weighted sum of

the individual model outputs. This final imputed value is computed as:

$$\widehat{y}_i = \omega_{lnn} \cdot \widehat{y}_i, lnn + \omega_{lstm} \cdot \widehat{y}_i, lstm \tag{16}$$

The weights ω_{lnn} and ω_{lstm} are computed based on the RMSE values obtained from the test data for each specific building type and missing data scenario. These weights are static within a dataset, meaning that for a given building type and missing rate, the same weights are applied to all imputed values. However, they are not globally fixed; instead, they are independently computed for each building type and missing data rate to reflect the unique characteristics of that dataset. Since energy consumption patterns vary substantially across commercial, residential, and hospital buildings and are further influenced by seasonal operational patterns, the RMSE values of the LNN and LSTM models differ across datasets. Therefore, the resulting weights ω_{lnn} and ω_{lstm} are recalculated for each dataset to optimize the imputation performance according to the building's temporal dynamics and operational characteristics. A similar method is used by Sun et al. [50], where inverse expected error variance is applied to improve ensemble accuracy in temperature forecasting. In our study, we adopt a comparable approach but use the inverse RMSE, serving as a practical proxy for model variance, to determine weights for combining predictions. This weighting strategy follows the broader principle of ensemble modeling practices, where inverse error-based weighting is employed to assign greater importance to models with higher predictive reliability. Additionally, the idea of weighting based on proximity to known data is conceptually aligned with inverse distance weighting (IDW) techniques used in time series imputation [50,51]. While IDW relies on spatial or temporal closeness, our framework instead assigns greater importance to the model with lower prediction error for a given data context thus generalizing the IDW logic to model selection. This design ensures that each dataset benefits from a weighting strategy tailored to its specific short-term and long-term dependencies, aligning with the distinct energy usage patterns and fluctuations present in different building types and seasons.

2.2. Data collection and pre-processing

This study used electricity consumption data obtained from the Advanced Metering Infrastructure (AMI) provided by the Korea Electric Power Corporation (KEPCO) for three building types: Type-A (commercial buildings), Type-B (residential buildings), and Type-C (hospitals). The dataset spans from January to December 2022 and records 15-min interval consumption data from buildings in Seoul and Gyeonggi-do, South Korea. Initially, nine buildings were considered for each category, totaling 27 sites. A minimum threshold of approximately 33,000 observations was applied to selected sites to minimize the impact of missing values. One representative building from each category was chosen which met this criterion, with 33,217 (Type-A), 33,309 (Type-B), and 33,022 (Type-C) observations.

Data preprocessing was carried out to ensure data suitability for analysis. The dataset was labeled with features reflecting temporal consumption patterns. A binary indicator denoted working hours and working days, assigned as 0 for non-working hours and weekdays, and 1 for working hours and weekends. General working hours (9AM - 6PM) were applied across all building types for simplicity in modelling, without additional segmentation for specific contexts like hospitals, which may include emergency rooms and inpatient operations. Seasonal variations were also encoded numerically (0 for winter, 1 for spring, 2 for summer, and 3 for autumn) to account for heating and cooling trends. Additionally, 'hour of the day' was label-encoded with its corresponding hour to capture daily consumption patterns.

To standardize the dataset, a standard scaler was applied, normalizing values to a mean of zero and standard deviation of one. The formula for standard scaler normalization is:

$$X_{\text{normalized}} = \frac{X - \mu}{\sigma} \tag{17}$$

where, for the $X_{\text{normalized}}$ value, X is the actual value while μ is the mean of the dataset and σ is the standard deviation of the dataset [52]. Post-imputation, the estimated values were rescaled using the inverse transformation and integrated back into the dataset to replace missing entries.

2.3. Introducing missing data

There are three methods for introducing missing data into a dataset: MCAR, Missing at Random (MAR), and Missing Not at Random (MNAR) [53,54]. To simulate real-life scenarios in datasets where missing data points are common, we purposefully generated missing data using the MCAR technique [55]. MCAR data is generated by randomly removing a specified proportion of values from a complete dataset, ensuring that the probability of missingness is independent of any observed or unobserved variables. This was achieved using a Bernoulli distribution, where each data point was assigned a "missing" or "not missing" status based on a specified probability [6,56]. We tested this method with three missing data levels (20 %, 30 %, and 40 %) to evaluate the imputation models' performance across varying degrees of data loss [57]. A copy of the original complete dataset was preserved as the ground truth for later evaluation. After applying MCAR, the dataset was divided into two subsets:

- Complete rows: Records with no missing values after MCAR application.
- Incomplete rows: Records with at least one missing value.

The complete rows were further split into training (80 %) and testing (20 %) subsets. The training subset was used to train the

imputation models, while the testing subset evaluated their generalization on fully observed data. Once trained, the models were applied to the incomplete rows to impute missing values. Finally, imputation performance was assessed by comparing the imputed values against the preserved ground truth in the incomplete rows using RMSE and Pearson's correlation coefficient.

2.4. Benchmark models

To identify the most effective approaches for data imputation, we conducted a comprehensive benchmarking study, evaluating a range of models from traditional ML techniques to advanced deep learning architectures. Basic ML techniques included Soft-Impute, which uses matrix completion, and KNN, which imputes via nearest neighbors, both leveraging data relationships for accuracy [56, 62]. For complex tasks, we tested RF (robust to outliers, captures non-linear patterns), SVM (effective for high-dimensional data), and MLP (flexible for non-linear, heterogeneous data) [56,62]. Advanced deep learning models such as Transformer networks (attention-based for long sequences) and LSTM (designed for temporal dependencies) were used to address time-series dynamics [63,64]. Lastly, LNNs, inspired by biological systems and adapts dynamically to evolving patterns, is also implemented for building energy imputation [41].

2.5. Model setup

The tests were carried out on a high-performance desktop computer equipped with a 13th Generation Intel Core i5-13400F CPU (2.50 GHz) and 64 GB of memory. The implementation and training of deep learning models were conducted using Python 3.9.0 and PyTorch 2.3.0 [58].

2.5.1. Hyperparameter optimization

The process of hyperparameter optimization was integral to ensuring the model's performance. A systematic grid search approach was employed to explore a range of hyperparameter combinations, such as learning rates, batch sizes, dropout rates, and architectural configurations.

The LNN model was configured with four hidden layers (32, 64, 32, and 32 neurons) and trained using the Adam optimizer with learning rates between 0.001 and 0.0001. Batch sizes of 32, 64, and 128 were tested, and a 0.2 dropout rate was applied to mitigate overfitting, with early stopping (patience = 20 epochs) to enhance efficiency [59]. The model underwent training for up to 250 epochs, leveraging an ODE Solver for temporal modeling. The LSTM model following a similar setup, consisted of four layers (64, 32, 128, 64 neurons) and was optimized using the same grid search methodology.

The Transformer model featured four layers (64, 128, 64, 128 neurons) with a multi-head self-attention mechanism, resulting in a high parameter count (520,193). In contrast, the MLP had four layers (100, 32, 32, 100 neurons) with a significantly lower parameter count (8,289), making it computationally efficient. Table 1 provides a comprehensive summary of the architectural configurations and parameter specifications for each deep learning model used in this study. Table S1 provides details on their computational performance, including training times and memory usage.

Alongside deep learning models, traditional ML were also tested. SoftImpute applied matrix factorization, while KNN (with k = 5) balanced bias-variance trade-offs for robustness. RF was tuned via grid search for hyperparameters like n-estimators (50–300), max depth (None, 10, 20, 30), and min samples split (2–10). SVM (LinearSVR) was optimized for regularization parameter C (0.1, 1, 10) and epsilon (0.01, 0.1, 1) to enhance predictive performance.

2.6. Implementing ILLWM

The implementation of ILLWM follows the framework outlined in Section 2.1.3 to impute missing values in energy consumption datasets. Using preprocessed data with missing values introduced at 20 %, 30 %, and 40 % via the MCAR technique, the process is carried out in three key steps. First, LNN and LSTM models independently generate imputation estimates for missing values. Next, the performance-based weighting mechanism is applied, where RMSE determines each model's contribution to the final imputed values. Finally, the imputed values are denormalized and integrated into the dataset, replacing missing entries. ILLWM's performance is then evaluated through RMSE and Pearson's correlation coefficient, as discussed in the next section.

Table 1
Comparison of layers and parameters of the deep learning models used.

Model	Input data (as sub-categorical features)	Number of neurons/ cells in each hidden layer	Number of hidden/encoder layers	Total number of layers	Total number of neurons (Input + hidden Output)	Total number of parameters (weights + bias)
LNN	5	32, 64, 32, 32	4	6	166	5473
LSTM	5	64, 32, 128, 64	4	6	326	59841
Transformer	5	64, 128, 64, 128	4	6	390	520193
MLP	5	100, 32, 32, 100	4	6	270	8289

2.7. Model evaluation

We used two main metrics to evaluate the performance of the chosen models: RMSE and Pearson Correlation Coefficient. The RMSE was computed to measure the average size of error between the estimated values and the real data. RMSE has the ability to measure the precision of predictive models, especially used in regression assignments to evaluate model performance. The RMSE formula is given by:

$$\mathrm{RMSE} = \sqrt{\frac{1}{n}\sum_{i=1}^{n}(y_i - \widehat{y_i})^2} \tag{18}$$

where, y_i is the real value while $\widehat{y_i}$ is imputed value and n is the number of observations. A lower RMSE value shows greater precision in the imputation procedure, assessing the efficiency and reliability of imputation models, as it indicates a less significant error between the imputed and observed values.

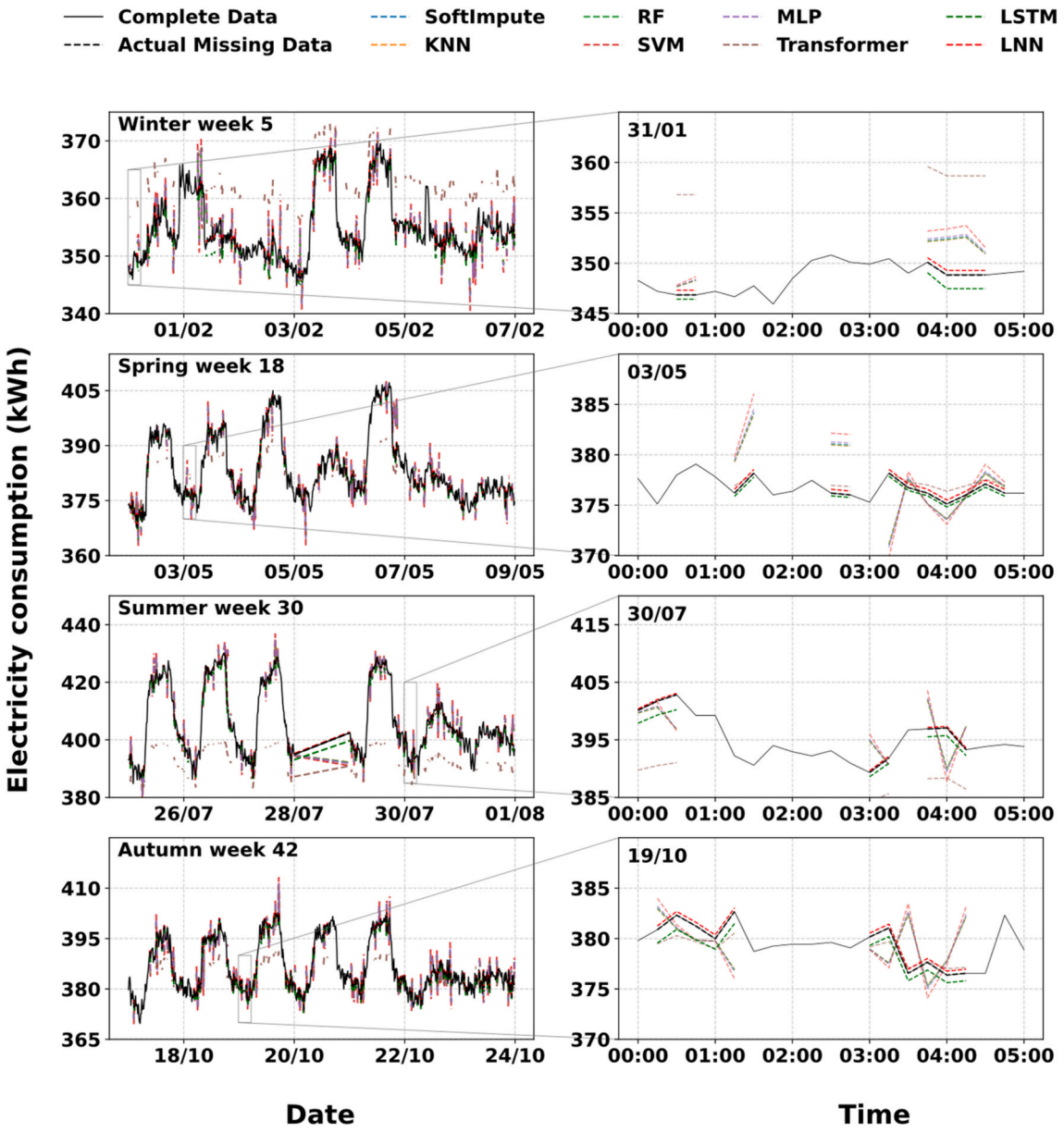

Fig. 3. Imputation values of electrical consumption in kWh for type A (commercial) buildings using different models when the missing values are introduced using MCAR at 40 %, missing rate.

As another metric to evaluate imputation accuracy, we computed the Pearson correlation coefficient to assess the linear association between the imputed and real data points. The formula used to calculate the Pearson correlation coefficient is as follows:

$$r = \frac{\sum_{i=1}^{n}(x_i - \bar{x})(y_i - \bar{y})}{\sqrt{\sum_{i=1}^{n}(x_i - \bar{x})^2 \sum_{i=1}^{n}(y_i - \bar{y})^2}} \tag{19}$$

where, r is the correlation coefficient, x_i and y_i are actual and imputed values respectively while $\bar{x}$ and $\bar{y}$ are the means of actual and imputed values respectively. A high value of correlation coefficient shows strong correlation which indicates that the imputed data effectively represents the connections found in the original dataset, preserving its integrity for further examination [60].

3. Results

3.1. Performance of the existing models

Fig. 3 shows a comparative analysis of various imputation methods for electricity consumption data across different seasons, with missing values introduced using the MCAR technique at a 40 % missing rate. The panels on the left depicts a representative week from each season, accompanied by zoomed-in views of a 6-h segment within a day from the corresponding week to emphasize model performance on the right.

The performance of various models, from simpler ML techniques to advanced neural networks, reveals distinct trends in their ability to handle missing energy consumption data. SoftImpute and KNN offer slight improvements, managing to approximate some peaks and troughs but still lagging during rapid changes, leading to over-smoothed results, particularly in spring and autumn. RF and SVM generally perform better, closely following consumption patterns and capturing peaks and troughs more effectively, though RF sometimes shows a minor delay in responding to rapid shifts. Advanced models, particularly the MLP and transformer, consistently align with the actual data and effectively capture seasonal patterns. The transformer model demonstrates strong responsiveness to sudden changes, especially during high-consumption fluctuations in summer and the dynamic usage patterns observed in spring. Neural network models, particularly LNN, excel across all seasons by capturing fine variations. While LSTM also performs well, it occasionally over-smooths some fluctuations, missing finer details that LNN effectively captures, especially during high-consumption periods.

Similarly, in the hourly snapshots, the simpler approach, such as SoftImpute, is consistently inadequate, underestimating variations and smoothing over critical peaks and valleys. KNN, RF, and SVM capture broader trends but miss finer details within hours. MLP and Transformer closely follow actual data, particularly during periods of rapid change in summer and winter, with Transformer being more adept at handling complex fluctuations. LNN provides the highest precision in this hourly analysis, capturing subtle changes, while LSTM closely follows but occasionally smooths certain peaks. Across all seasons, the LNN imputation model consistently performs best, accurately capturing both weekly trends and hourly details. LSTM follows closely, providing strong performance but occasionally smoothing over small fluctuations. Transformer and MLP also show robust performance, particularly in their responsiveness to sudden changes, although they do not match the accuracy of LNN and LSTM.

Table 2 provides a comparative analysis of RMSE across the evaluated models. The results demonstrate that LNN and LSTM consistently achieved the lowest RMSE scores across all building types (A: Commercial, B: Residential, C: Hospital). For Type A buildings, both models significantly outperformed traditional ML models and advanced imputation techniques, particularly at higher missing rates, with LNN and LSTM achieving RMSEs as low as 0.440. Similarly, for Type B buildings, LNN and LSTM showed superior performance, yielding much lower RMSEs compared to methods like RF and MLP with LNN and LSTM scoring as low as 0.16. For Type C buildings, LSTM and LNN continued to excel, achieving RMSEs as low as 0.29 and 0.21, respectively, at high missing rates. These results confirm that LNN and LSTM are highly effective for handling complex temporal dependencies in energy consumption data, establishing them as suitable models for missing data imputation under MCAR conditions.

Table 2
Comparison of RMSE of different imputation methods across building types and missing rates.

Building type	Missing rate	Imputation Package		Traditional ML			Advanced ML		LNN
		Soft Impute	KNN	RF	SVM	MLP	Transformer	LSTM	
Type A	0.2	10.01	8.45	8.14	12.03	10.03	7.61	0.55	0.24
	0.3	11.06	10.65	11.43	13.43	11.72	6.85	0.29	0.17
	0.4	12.33	11.87	12.04	15.89	12.98	8.5	0.98	0.44
Type B	0.2	55.03	51.42	53.65	55.37	45.21	65.08	0.61	0.1
	0.3	68.84	60.67	61.65	63.39	50.54	71.12	0.54	0.35
	0.4	79.94	71.44	72.77	71.07	60.64	71.74	0.41	0.16
Type C	0.2	29.1	27.43	29.16	30.01	25.67	33.1	0.78	0.69
	0.3	35.33	30.32	31.43	36.17	26.35	30.71	0.29	0.16
	0.4	41.02	35.2	38.01	37.04	34.2	32.43	0.29	0.21

3.2. Integrated LNN-LSTM weighted model

In this study, the novel proposed model, ILLWM, combined the strengths of both LNN and LSTM by summing their weighted imputed values, leveraging the advantages of each model. Fig. 4 shows a detailed comparison of the LNN model, LSTM model and the proposed ILLWM for electricity consumption data across four representative weeks from each season for type A buildings at 40 % missing rate. A zoomed-in view of a 5-h segment from a day within each week is displayed alongside the corresponding week.

Throughout the seasons, the ILLWM demonstrates adaptability and accuracy in imputing electricity consumption data by combining the strengths of both LSTM and LNN. In winter, where demand is stable, ILLWM effectively tracks minor fluctuations. For instance, on January 31, when consumption dropped from 350.1 kWh (3:45 a.m.) to 348.84 kWh (4:30 a.m.), ILLWM predicted 350.092 kWh and 348.734 kWh, closer to the observed values than LNN (350.554 kWh, 349.300 kWh) or LSTM (349.069 kWh,

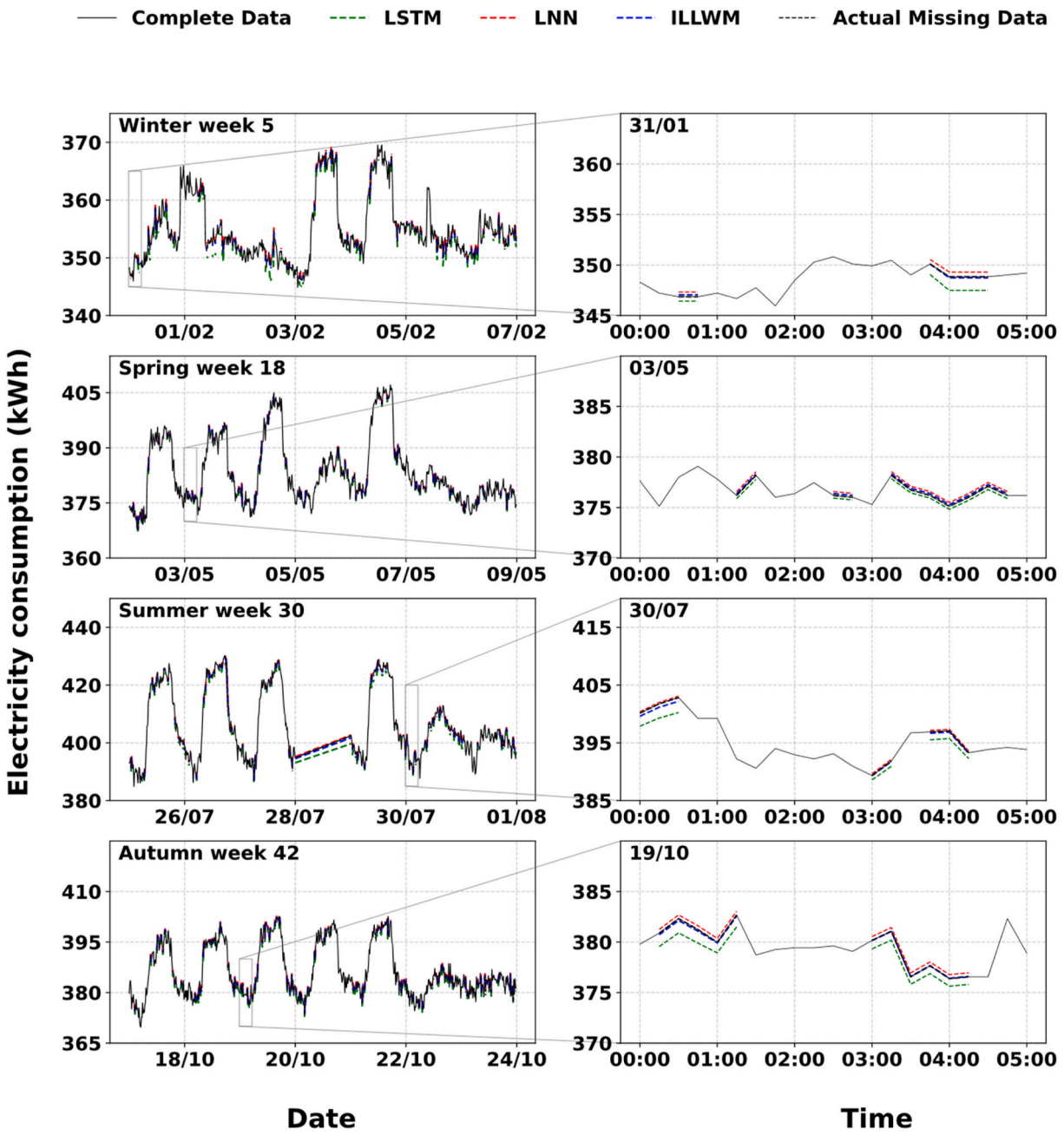

Fig. 4. Imputed electrical consumption values (in kWh) for Type A (commercial) buildings using the standalone LNN model, LSTM model, and the proposed ILLWM, with missing values introduced at a 40 % rate using the MCAR technique.

347.480 kWh). In spring, with more pronounced peaks and valleys, ILLWM accurately captured rapid changes. On May 3, when consumption dropped from 378.18 kWh (3:15 a.m.) to 375.12 kWh (4:00 a.m.), ILLWM predicted 378.34 kWh and 375.29 kWh, outperforming LNN (378.55 kWh, 375.51 kWh) and LSTM (377.86 kWh, 374.83 kWh). In summer, with frequent fluctuations, ILLWM effectively followed sudden shifts. On July 30, when demand rose from 400.14 kWh (12:00 a.m.) to 402.84 kWh (12:30 a.m.), ILLWM closely estimated 399.62 kWh and 402.20 kWh, outperforming LNN (400.40 kWh, 403.08 kWh) and LSTM (397.89 kWh, 400.25 kWh). Autumn shows patterns similar to spring, and ILLWM performed better in this season, too. On October 19, when consumption varied from 380.16 kWh (3:00 a.m.) to 376.38 kWh (4:00 a.m.), ILLWM predicted 380.16 kWh and 376.42 kWh, performing better than LNN (380.54 kWh, 376.78 kWh) and LSTM (379.33 kWh, 375.63 kWh).

Similar results are observed for Type B and Type C buildings, as shown in Figs. S1 and S2, respectively. For Type B buildings, which exhibit more stable energy consumption patterns compared to commercial or hospital buildings, the ILLWM consistently shows improvements over the standalone models. The combination of both models provides imputed values that are closer to the actual consumption values, leading to more accurate imputation, though the performance gains are less pronounced than in Type A or Type C buildings due to the lower variability in the data. In Type C buildings (hospitals), the ILLWM demonstrates the most significant performance improvements by effectively managing both short-term operational fluctuations (captured by LNN) and broad patterns driven by hospital schedules and critical equipment use (modeled by LSTM).

3.3. Improved imputation accuracy across building types

The results of the comparison of RMSE between the standalone LSTM, LNN, and the newly proposed ILLWM for type A, B, and C buildings at 20 %, 30 %, and 40 % missing rates are shown in Fig. 5. ILLWM consistently outperforms the standalone models. In Type A buildings, ILLWM achieves an RMSE of 0.102, significantly lower than LSTM's 0.977 and LNN's 0.440, with an improvement of 89.6 % over LSTM and 76.9 % over LNN (Fig. 5a). For Type B buildings (Fig. 5b), the ILLWM again outperforms the standalone models across all missing rates, with an RMSE of 0.130 which is 68.3 % lower than LSTM's 0.411 and 12 % lower than LNN's 0.148. Even though the

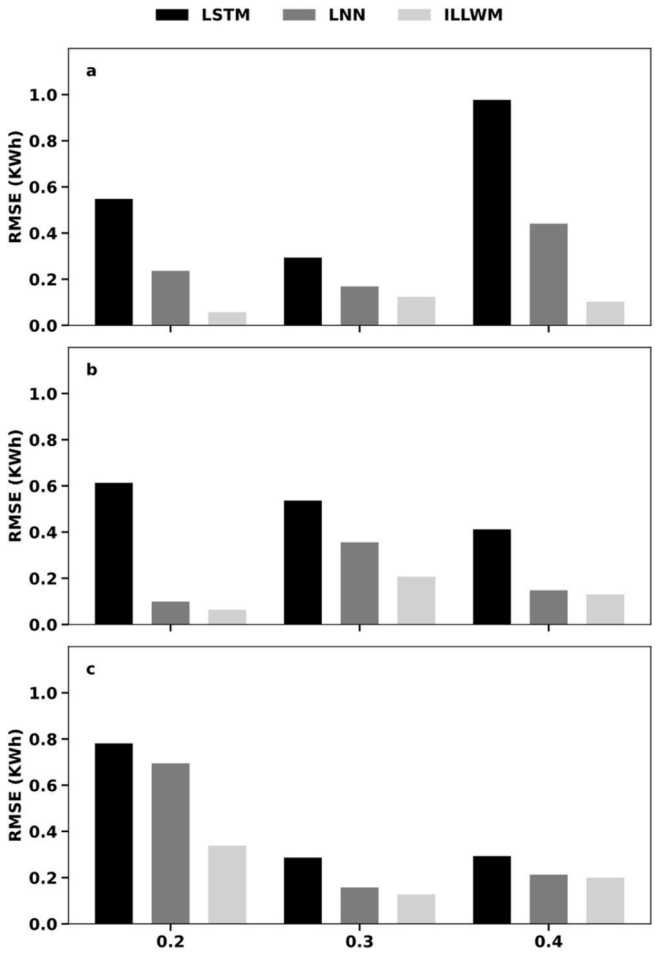

Fig. 5. RMSE between the standalone LSTM, LNN, and the newly proposed ILLWM for a. type A – residential buildings, b. type B – commercial buildings, and c. type C – hospital buildings.

gains are more modest in this case, the ILLWM consistently shows the lowest RMSE. In Type C buildings (Fig. 5c), the ILLWM provides the best performance across the board with an RMSE of 0.199. This represents a 31.9 % reduction in error compared to LSTM, which has an RMSE of 0.293, and a 6.1 % improvement over LNN's RMSE of 0.212. Here, the LSTM model encounters the highest RMSE, especially at the 0.4 missing rate, while the LNN performs better but still cannot match the ILLWM's accuracy. These results highlight the strength of the weighted model in handling missing data in more complex settings such as hospitals. The ILLWM consistently provided the closest imputation results to the actual missing data, particularly for commercial and hospital buildings, achieving significant reductions in RMSE.

Similarly, the correlation coefficient scores in Table 3 highlight the ILLWM's strong performance across all missing rates and building types. For instance, in type-B building, ILLWM achieves the highest correlation score of 0.9957 at a 40 % missing rate, outperforming MLP (0.7828) and Transformer ML (0.9138). In type-A building, ILLWM maintains a correlation of 0.9968 at 40 % missingness, surpassing MLP (0.7828) and Transformer ML (0.9438). For hospital buildings, ILLWM achieves 0.9996 correlation at the 40 % missing rate, outperforming KNN (0.772) and SVM (0.789). These results demonstrate ILLWM's effectiveness in handling complex, non-stationary datasets, particularly under MCAR conditions.

4. Discussion

4.1. Improvement in imputation with integrated LNN-LSTM weighted model

The study proposes a new ILLWM for imputing missing values in energy consumption datasets. The model demonstrates superior performance across different building types, and temporal variations. The performance of the model was evaluated using statistical analysis, particularly RMSE and Pearson's correlation coefficient compared to the standalone models. One of the key strengths of ILLWM is its ability to handle dynamic energy consumption datasets, which are influenced by factors such as seasonal changes, time of day, and regional variations [59–61]. Prior ML models, such as RF, SVM, and MLP, have shown moderate success at lower missing rates (up to 30 %) but tend to struggle with temporal dependencies at higher missing rates [62]. These models perform adequately under simpler conditions but demonstrate limited effectiveness in handling complex, structured missing data scenarios in energy datasets [21,63,64], [65].

The monthly and daily RMSE variability represented in Fig. 6a shows the model's temporal stability. For commercial building, the model maintains stable RMSE values throughout the year, with only slight increases in January and February under MCAR conditions, likely due to increased heating demands. However, hospital buildings experience more fluctuations, particularly a spike in RMSE in November, potentially due to operational changes and heightened energy demands during seasonal transitions. These results highlight the model's adaptability in managing diverse building types and consumption patterns while imputing missing values [14,66]. Moreover, day-wise analysis (Fig. 6 b) shows that hospital building experience spikes in RMSE on Fridays and Saturdays, suggesting more complex energy patterns toward the end of the week. Despite these fluctuations, ILLWM consistently outperforms traditional imputation methods, which often fail to capture such irregularities in energy consumption patterns [4,5]. The phenomenon of LSTM underestimating energy consumption, as reported by Ghanim et al. (2022) and Prater et al. (2024) [67], [68], and LNN overestimating energy consumption, as noted by Antonesi et al.(2025) [69], reflects their architectural differences. LSTM, designed for long-term temporal modeling [70], tends to smooth out short-term fluctuations, leading to underestimation of sharp consumption peaks. In contrast, LNN, which leverages continuous-time dynamics, responds more strongly to rapid variations [37]. These behaviors are consistently observed across different building types and missing data rates because they originate from the models' intrinsic learning biases. Rather than applying a static offset or fixed weighting, ILLWM computes dataset-specific weights (once during testing for each building type and missing rate), ensuring that imputation adapts to the operational and data completeness characteristics of each dataset. These weights remain constant during inference for that dataset, optimizing both performance and computational efficiency.

The RMSE values generally increase with higher missing data rates for most cases (Fig. 5), as noted in some previous studies [27, 71]. However, for commercial buildings, there is a drop in RMSE as the missing data rate increases. This behavior could be attributed to the proposed ILLWM architecture, which combines the strengths of LNN and LSTM networks and adjusts the weight of each component. Since the ILLWM does not undergo any architectural shift as the missingness increases, particularly in the case of

Table 3
Correlation coefficients between real and imputed data across building types using various imputation methods.

Building type	Missing rate	Imputation Package		Traditional ML			Advanced ML		LNN	ILLWM
		Soft Impute	KNN	RF	SVM	MLP	Transformer	LSTM		
Type A	0.2	0.8589	0.8698	0.8769	0.8769	0.8769	0.9684	0.982	0.9858	0.9966
	0.3	0.8088	0.8372	0.8271	0.8272	0.8272	0.9251	0.9835	0.9897	0.9982
	0.4	0.7995	0.7928	0.7828	0.7828	0.7828	0.9138	0.9706	0.9741	0.9989
Type B	0.2	0.8805	0.8698	0.8769	0.8769	0.8769	0.9084	0.9742	0.979	0.9898
	0.3	0.8309	0.8372	0.8271	0.8272	0.8272	0.9451	0.9926	0.9988	0.999
	0.4	0.7989	0.7928	0.7828	0.7828	0.7828	0.9438	0.9797	0.9896	0.9968
Type C	0.2	0.8789	0.8934	0.8934	0.8998	0.9087	0.9743	0.991	0.9975	0.9989
	0.3	0.8325	0.841	0.841	0.8548	0.8986	0.9686	0.9779	0.9989	0.9903
	0.4	0.7895	0.772	0.772	0.7895	0.8754	0.9361	0.9703	0.989	0.9996

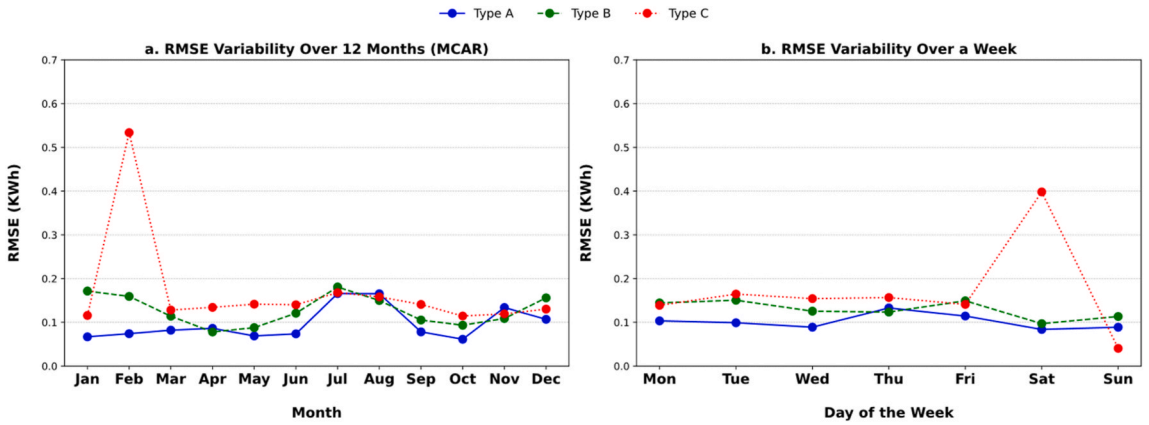

Fig. 6. RMSE variability over months and days of the week at maximum 40 % missing rate.

commercial buildings, the data distribution follows a pattern where the weighted model assigns more weight to the component that effectively captures trends under higher missing rates [50,51]. Additionally, the model is designed to generalize effectively with less available data, avoiding overfitting and resulting in lower RMSE values and more accurate imputation. Overall, the RMSE trends clearly demonstrate the reliability and consistency of the ILLWM across different building types and missing data scenarios.

4.2. Implications of the integrated LNN-LSTM weighted model

By combining LNN's ability to capture sudden fluctuations and long-term patterns, and LSTM's performance in handling temporal dependencies, ILLWM addresses a critical gap in the literature, the handling of non-stationary data with high missing rates. Traditional models often fail to capture both short-term fluctuations and long-term trends simultaneously, particularly in dynamic environments like building energy management [34,35]. ILLWM's integrated weighting mechanism bridges this gap, ensuring that the model adapts to the characteristics of the data, and thereby improving imputation performance [72,73]. The ILLWM's better performance in data imputation has significant implications for building energy management. By improving the quality of imputed data, the ILLWM enables more reliable energy analytics, enhances demand-side forecasting, reduces operational costs, and supports improved control decisions within BEMS [26,27,74]. Practically, the model can be embedded into real-time energy monitoring infrastructures to continuously correct missing or faulty readings from smart meters and sensors. This makes ILLWM highly suitable for deployment in commercial buildings, residential complexes, and healthcare facilities where uninterrupted, accurate energy data is essential for efficient facility operation and fault detection.

Moreover, by integrating LNN and LSTM, the ILLWM achieves a balance between accuracy and efficiency. Among the models evaluated, MLP and LNN are inherently more computationally efficient due to their lower parameter counts and simpler architectures, as demonstrated in Table 1. However, our study highlights that while LNN and LSTM outperform other models such as MLP and traditional ML techniques in imputation accuracy, they are also significantly more effective than computationally heavier models like Transformers. The computational efficiency of ILLWM is particularly advantageous for real-world applications where resource constraints, such as limited processing power or the need for real-time predictions, are critical. This efficiency makes it especially suitable for energy consumption datasets, which often involve large-scale and dynamic data with high variability [75]. The computational efficiency of ILLWM is particularly advantageous for real-world building applications, where constraints such as limited edge computing capacity or the need for real-time predictions may exist. This makes it feasible for integration into cloud-based dashboards, edge devices, or energy auditing platforms [76]. Its scalability and computational efficiency make it an ideal tool for applications in energy monitoring, forecasting, anomaly detection and management, especially in dynamic, real-world environments where data completeness is often a challenge [77].

4.3. Limitations

While our study demonstrated better imputation performance, some limitations must be acknowledged. First, the scope was restricted to specific building types and regions in South Korea, which may limit the generalizability of our findings to other settings with different energy consumption profiles [78]. Additionally, the model's performance under MAR and MNAR conditions was not evaluated, and the hyperparameter optimization was relatively constrained. Future research should expand scope by utilizing larger and more diverse datasets from various global regions, assessing the model's performance under MAR and MNAR scenarios, and apply more advanced hyperparameter optimization techniques [79]. Furthermore, improving computational efficiency, exploring alternative ODE solvers, and testing the model's robustness to noise are essential for its practical deployment. Integrating the ILLWM network with other advanced imputation methods, as well as utilizing Neural Architecture Search (NAS) to optimize model architectures, could further improve performance.

5. Conclusions

This study introduced a novel imputation model, ILLWM, designed to address the challenge of missing data in energy consumption datasets. By leveraging the adaptive capabilities of LNN and the temporal strength of LSTM networks, the model delivers a scalable and efficient solution for time-series imputation in energy management. The primary objective was to enhance imputation accuracy across various building types using MCAR missing data mechanism by weighting the contributions of LNN and LSTM models. The results consistently showed that the ILLWM demonstrated better performance than traditional ML methods and advanced ML models. The model achieved lower RMSE values, achieving significant RMSE reductions, especially for commercial buildings (76.9 % over LNN and 89.6 % over LSTM with 40 % missing data). Hospital buildings showed a notable improvement, with a 6.12 % reduction over LNN and 31.93 % over LSTM. The ILLWM's adaptability to dynamic energy data allows it to maintain improved imputation accuracy across different missing data rates. The high Pearson correlation scores further underscore the model's capability to preserve the original data structure, ensuring that imputed values align closely with the actual energy consumption patterns. These results are critical for applications such as load forecasting and energy demand management, where the integrity of time-series data is paramount. These results demonstrate the potential of the ILLWM to significantly enhance data reliability, fostering more accurate energy demand forecasting and supporting the development of sustainable energy management strategies across diverse building environments. By ensuring the completeness and accuracy of datasets, the model contributes to improved decision-making processes in real-time energy applications. Its computational efficiency, driven by the integrated weighting mechanism, minimizes the need for frequent retraining, making it particularly suitable for dynamic scenarios where data updates are frequent and missing values are prevalent. This capability enables stakeholders to optimize resource allocation, plan for future energy needs, and implement innovative strategies to achieve energy efficiency and sustainability objectives effectively.

CRediT authorship contribution statement

Saeed Murtaza: Writing – original draft, Validation, Software, Investigation, Formal analysis, Data curation. **Sarath Raj:** Writing – review & editing, Writing – original draft, Formal analysis. **Geun Young Yun:** Writing – review & editing, Writing – original draft, Supervision, Methodology, Funding acquisition, Conceptualization. **Duk-Joon Park:** Writing – review & editing, Resources. **Ji-Hye Kim:** Writing – review & editing, Resources. **Gwanyong Park:** Writing – review & editing, Resources. **Jin Woo Moon:** Writing – review & editing, Resources.

Declaration of competing interest

The authors declare that they have no known competing financial interests or personal relationships that could have appeared to influence the work reported in this paper.

Acknowledgements

This work was supported by the National Research Foundation of Korea (NRF) grant funded by the Korea government (MSIT) (RS-2025-00554879). This work was supported by the National Research Foundation of Korea (NRF) grant funded by the Korea government (MSIT) (No. RS-2023-00217322).

Appendix A. Supplementary data

Supplementary data to this article can be found online at https://doi.org/10.1016/j.jobe.2025.113774.

Data availability

The data that has been used is confidential.

References

[1] S. Jeong, Y.M. Wi, Research on development and implementation of integrated energy management system for buildings, J. Electrical Eng. Technol. (2024), https://doi.org/10.1007/s42835-024-01870-3.
[2] B. Farhadi, J. You, D. Zheng, L. Liu, S. Wu, J. Li, et al., Machine learning for fast development of advanced energy materials, Next Mater. 1 (2023) 100025, https://doi.org/10.1016/j.nxmate.2023.100025.
[3] S. Jang, S.-J. Shin, Deep learning-based smart meter wattage prediction analysis platform, Int. J. Adv. Smart Convergence 9 (2020) 173–178, https://doi.org/10.7236/IJASC.2020.9.4.173.
[4] I. Izonin, N. Kryvinska, R. Tkachenko, K. Zub, An approach towards missing data recovery within IoT smart system, Procedia Comput. Sci. 155 (2019) 11–18, https://doi.org/10.1016/j.procs.2019.08.006. Elsevier B.V.
[5] R. Yuan, S.A. Pourmousavi, W.L. Soong, A.J. Black, J.A.R. Liisberg, J. Lemos-Vinasco, Unleashing the benefits of smart grids by overcoming the challenges associated with low-resolution data, Cell Rep. Phys. Sci. 5 (2024), https://doi.org/10.1016/j.xcrp.2024.101830.
[6] Y. Dong, C.Y.J. Peng, Principled missing data methods for researchers, SpringerPlus 2 (2013) 1–17, https://doi.org/10.1186/2193-1801-2-222/TABLES/3.

[7] M.C. Wang, C.F. Tsai, W.C. Lin, Towards missing electric power data imputation for energy management systems, Expert Syst. Appl. 174 (2021) 114743, https://doi.org/10.1016/J.ESWA.2021.114743.
[8] T. Kim, W. Ko, J. Kim, Analysis and impact evaluation of missing data imputation in day-ahead PV generation forecasting, Appl. Sci. (Switzerland) 9 (2019), https://doi.org/10.3390/APP9010204.
[9] D.S. Bräm, U. Nahum, A. Atkinson, G. Koch, M. Pfister, Evaluation of machine learning methods for covariate data imputation in pharmacometrics, CPT Pharmacometrics Syst. Pharmacol. 11 (2022) 1638–1648, https://doi.org/10.1002/psp4.12874.
[10] I. Mayer, A. Sportisse, J. Josse, N. Tierney, N. Vialaneix, R-miss-tastic: a unified platform for missing values methods and workflows, ArXiv Preprint (2019).
[11] M. Wolbers, A. Noci, P. Delmar, C. Gower-Page, S. Yiu, J.W. Bartlett, Standard and reference-based conditional mean imputation, Pharm. Stat. 21 (2022), https://doi.org/10.1002/pst.2234.
[12] R.R. Andridge, R.J.A. Little, A review of hot deck imputation for survey non-Response, Int. Stat. Rev. 78 (2010) 40, https://doi.org/10.1111/J.1751-5823.2010.00103.X.
[13] M.I. Mohd Jaya, Cold Deck Missing Value Imputation with a Trust-based Selection Method of Multiple Web Donors, Universiti Putra Malaysia, 2018.
[14] D.P. Petersen, D. Middleton, Linear interpolation, extrapolation, and prediction of random space-time fields with a limited domain of measurement, IEEE Trans. Inf. Theor. 11 (1965) 18–30, https://doi.org/10.1109/TIT.1965.1053734.
[15] B.R. Winck, J.M.G. Bloor, K. Klumpp, Eighteen years of upland grassland carbon flux data: reference datasets, processing, and gap-filling procedure, Sci. Data 10 (2023), https://doi.org/10.1038/s41597-023-02221-z.
[16] E.L. Silva-Ramírez, R. Pino-Mejías, M. López-Coello, M.D. Cubiles-de-la-Vega, Missing value imputation on missing completely at random data using multilayer perceptrons, Neural Netw. 24 (2011) 121–129, https://doi.org/10.1016/j.neunet.2010.09.008.
[17] V. Hassija, V. Chamola, A. Mahapatra, A. Singal, D. Goel, K. Huang, et al., Interpreting black-box models: a review on explainable artificial intelligence, Cognit Comput. 16 (2024) 45–74, https://doi.org/10.1007/s12559-023-10179-8.
[18] J.H. Li, S.X. Guo, R.L. Ma, J. He, X.H. Zhang, D.S. Rui, et al., Comparison of the effects of imputation methods for missing data in predictive modelling of cohort study datasets, BMC Med. Res. Methodol. 24 (2024), https://doi.org/10.1186/s12874-024-02173-x.
[19] F. Lalande, K. Doya, Numerical Data Imputation for Multimodal Data Sets: a Probabilistic Nearest-Neighbor Kernel Density Approach, 2023.
[20] L.A. Wang, R. Kern, E. Yu, S. Choi, J.Q. Pan, IntelliSleepScorer, a software package with a graphic user interface for automated sleep stage scoring in mice based on a light gradient boosting machine algorithm, Sci. Rep. 13 (2023), https://doi.org/10.1038/s41598-023-31288-2.
[21] Q. Yao, J.T. Kwok, Accelerated and inexact soft-impute for large-scale matrix and tensor completion, IEEE Trans. Knowl. Data Eng. 31 (2019) 1665–1679, https://doi.org/10.1109/TKDE.2018.2867533.
[22] Y. Sun, J. Li, Y. Xu, T. Zhang, X. Wang, Deep learning versus conventional methods for missing data imputation: a review and comparative study, Expert Syst. Appl. 227 (2023), https://doi.org/10.1016/j.eswa.2023.120201.
[23] O. Valenzuela, A. Catala, D. Anguita, I. Rojas, New advances in artificial neural networks and machine learning techniques, Neural Process. Lett. 55 (2023) 5269–5272, https://doi.org/10.1007/s11063-023-11350-w.
[24] F. Xiao, C. Fan, Data mining in building automation system for improving building operational performance, Energy Build. 75 (2014) 109–118, https://doi.org/10.1016/J.ENBUILD.2014.02.005.
[25] L. Zhang, A pattern-recognition-based ensemble data imputation framework for sensors from building energy systems, Sensors 20 (2020) 5947, https://doi.org/10.3390/S20205947, 2020;20:5947.
[26] D. Jeong, C. Park, Y.M. Ko, Missing data imputation using mixture factor analysis for building electric load data, Appl. Energy 304 (2021) 117655, https://doi.org/10.1016/J.APENERGY.2021.117655.
[27] J. Ma, J.C.P. Cheng, F. Jiang, W. Chen, M. Wang, C. Zhai, A bi-directional missing data imputation scheme based on LSTM and transfer learning for building energy data, Energy Build. 216 (2020) 109941, https://doi.org/10.1016/J.ENBUILD.2020.109941.
[28] C. Fu, M. Quintana, Z. Nagy, C. Miller, Filling time-series gaps using image techniques: multidimensional context autoencoder approach for building energy data imputation, Appl. Therm. Eng. 236 (2024) 121545, https://doi.org/10.1016/J.APPLTHERMALENG.2023.121545.
[29] J. Yang, K.K. Tan, M. Santamouris, S.E. Lee, Building energy consumption raw data forecasting using data cleaning and deep recurrent neural networks, Buildings 9 (2019) 204, https://doi.org/10.3390/BUILDINGS9090204, 2019;9:204.
[30] A. Liguori, R. Markovic, M. Ferrando, J. Frisch, F. Causone, C. van Treeck, Augmenting energy time-series for data-efficient imputation of missing values, Appl. Energy 334 (2023) 120701, https://doi.org/10.1016/J.APENERGY.2023.120701.
[31] A. Liguori, M. Quintana, C. Fu, C. Miller, J. Frisch, C. van Treeck, Opening the black box: towards inherently interpretable energy data imputation models using building physics insight, Energy Build. 310 (2024) 114071, https://doi.org/10.1016/J.ENBUILD.2024.114071.
[32] Z. Wang, L. Wang, Y. Tan, J. Yuan, Fault detection based on Bayesian network and missing data imputation for building energy systems, Appl. Therm. Eng. 182 (2021) 116051, https://doi.org/10.1016/J.APPLTHERMALENG.2020.116051.
[33] R. Wu, S.D. Hamshaw, L. Yang, D.W. Kincaid, R. Etheridge, A. Ghasemkhani, Data imputation for multivariate time series sensor data with large gaps of missing data, IEEE Sens. J. 22 (2022) 10671–10683, https://doi.org/10.1109/JSEN.2022.3166643.
[34] I.H. Sarker, Deep learning: a comprehensive overview on techniques, taxonomy, applications and research directions, SN Comput Sci. 2 (2021), https://doi.org/10.1007/s42979-021-00815-1.
[35] F.A. Adnan, K.R. Jamaludin, W.Z.A. Wan Muhamad, S. Miskon, A review of the current publication trends on missing data imputation over three decades: direction and future research, Neural Comput. Appl. 34 (2022) 18325–18340, https://doi.org/10.1007/s00521-022-07702-7.
[36] R.M. Hasani, M. Lechner, A. Amini, D. Rus, R. Grosu, Liquid time-constant recurrent neural networks as universal approximators, ArXiv Preprint (2018).
[37] R. Hasani, M. Lechner, A. Amini, D. Rus, R. Grosu, Liquid time-constant networks. Proceedings of the AAAI Conference on Artificial Intelligence, Association for the Advancement of Artificial Intelligence, 2021, pp. 7657–7666, https://doi.org/10.1609/AAAI.V35I9.16936, 35.
[38] D. Das, S. Bhattacharya, U. Pal, S. Chanda, PLSM: a Parallelized Liquid State Machine for Unintentional Action Detection, 2021.
[39] M. Bidollahkhani, F. Atasoy, H. Abdellatef, LTC-SE: expanding the potential of liquid time-constant neural networks for scalable AI and embedded systems, ArXiv Preprint (2023).
[40] J.G. White, E. Southgate, J.N. Thomson, S. Brenner, The Structure of the Nervous System of the Nematode Caenorhabditis elegans, vol 314, 1986.
[41] D.G. Albertson, J.N. Thomson, The pharynx of Caenorhabditis elegans, Philos. Trans. R. Soc. Lond. B Biol. Sci. 275 (1976) 299–325, https://doi.org/10.1098/RSTB.1976.0085.
[42] M. Lechner, R. Hasani, A. Amini, T.A. Henzinger, D. Rus, R. Grosu, Neural circuit policies enabling auditable autonomy, Nat. Mach. Intell. 2 (2020) 642–652, https://doi.org/10.1038/s42256-020-00237-3.
[43] P. Gajjar, A. Saxena, K. Acharya, P. Shah, C. Bhatt, T.T. Nguyen, Liquidt: stock market analysis using liquid time-constant neural networks, Int. J. Inf. Technol. 16 (2024) 909–920, https://doi.org/10.1007/s41870-023-01506-1.
[44] X. Wang, F. Zhu, C. Huang, A. Alhammadi, F. Bader, Z. Zhang, et al., Robust beamforming with gradient-based liquid neural network, IEEE Wireless Commun. Lett. (2024) 1–5, https://doi.org/10.48550/arXiv.2405.07291.
[45] W.A. Pawlak, M. Isik, D. Le, I.C. Dikmen, Exploring liquid neural networks on Loihi-2, ArXiv Preprint 1–8 (2024), https://doi.org/10.48550/arXiv.2407.20590.
[46] B. Xu, N. Wang, T. Chen, M. Li, Empirical Evaluation of Rectified Activations in Convolutional Network, 2015.
[47] C. Leo, The math behind LSTM. https://medium.com/towards-data-science/the-math-behind-lstm-9069b835289d, 2024. (Accessed 3 February 2025).
[48] F. Landi, L. Baraldi, M. Cornia, R. Cucchiara, Working memory connections for LSTM, Neural Netw. 144 (2021), https://doi.org/10.1016/j.neunet.2021.08.030.
[49] S. Mahjoub, L. Chrifi-Alaoui, B. Marhic, L. Delahoche, Predicting energy consumption using LSTM, multi-layer GRU and Drop-GRU neural networks, Sensors 22 (2022) 4062, https://doi.org/10.3390/S22114062, 2022;22:4062.
[50] X. Sun, J. Yin, Y. Zhao, Using the inverse of expected error variance to determine weights of individual ensemble members: application to temperature prediction, J. Meteorological Res. 31 (2017) 502–513, https://doi.org/10.1007/S13351-017-6047-0/METRICS.

[51] Dhevi AT. Sree, Imputing missing values using inverse distance weighted interpolation for time series data. 6th International Conference on Advanced Computing, ICoAC, 2014, pp. 255–259, https://doi.org/10.1109/ICOAC.2014.7229721, 2015.
[52] T. Hastie, R. Tibshirani, J. Friedman, The Elements of Statistical Learning Data Mining, Inference, and Prediction, 2009.
[53] D.B. Rubin, Inference and missing data, Biometrika 63 (1976) 581, https://doi.org/10.2307/2335739.
[54] R.J.A. Little, D.B. Rubin, Statistical Analysis with Missing Data, wiley, 2002, https://doi.org/10.1002/9781119013563.
[55] C. Li, Little's test of missing completely at random, STATA J. 13 (2013) 795–809.
[56] M.S. Santos, R.C. Pereira, A.F. Costa, J.P. Soares, J. Santos, P.H. Abreu, Generating synthetic missing data: a review by missing mechanism, IEEE Access 7 (2019) 11651–11667, https://doi.org/10.1109/ACCESS.2019.2891360.
[57] Z. Ghahramani, M.I. Jordan, Supervised learning from incomplete data via an EM approach, Adv. Neural Inf. Process. Syst. 6 (NIPS 1993) (1993) 120–127.
[58] A. Paszke, S. Gross, F. Massa, A. Lerer, J. Bradbury Google, G. Chanan, et al., Pytorch: an imperative style, high-performance deep learning library, Adv. Neural Inf. Process. Syst. (2019).
[59] D.P. Kingma, J.L. Ba, Adam: a method for stochastic optimization, ArXiv Preprint (2014).
[60] J. Cohen, Statistical Power Analysis for the Behavioral Sciences, 1988. New York.
[61] G. Chen, S. Lu, S. Zhou, Z. Tian, M.K. Kim, J. Liu, et al., A systematic review of building energy consumption prediction: from perspectives of load classification, data-driven frameworks, and future directions, Appl. Sci. 15 (2025) 3086, https://doi.org/10.3390/APP15063086, 2025;15:3086.
[62] S. Bhanja, S. Metia, A. Das, A smart city air quality data imputation method using markov weights-based fuzzy transfer learning, IETE J. Res. 69 (2023) 5755–5763, https://doi.org/10.1080/03772063.2023.2186500.
[63] F. Lalande, K. Doya, Numerical Data Imputation for Multimodal Data Sets: a Probabilistic Nearest-Neighbor Kernel Density Approach, 2023.
[64] L.A. Wang, R. Kern, E. Yu, S. Choi, J.Q. Pan, IntelliSleepScorer, a software package with a graphic user interface for automated sleep stage scoring in mice based on a light gradient boosting machine algorithm, Sci. Rep. 13 (2023), https://doi.org/10.1038/s41598-023-31288-2.
[65] C. Miller, B. Picchetti, C. Fu, J. Pantelic, Limitations of machine learning for building energy prediction: ASHRAE great energy predictor III kaggle competition error analysis, Sci. Technol. Built Environ. 28 (2022) 610–627, https://doi.org/10.1080/23744731.2022.2067466.
[66] H. Dhungana, F. Bellotti, R. Berta, A. De Gloria, Performance comparison of imputation methods in building energy data sets, Lecture Notes Electrical Eng. 738 (2021) 144–151, https://doi.org/10.1007/978-3-030-66729-0_17.
[67] J. Ghanim, M. Issa, M. Awad, An asymmetric loss with anomaly detection LSTM framework for power consumption prediction. MELECON 2022 - IEEE Mediterranean Electrotechnical Conference, Proceedings, 2022, pp. 819–824, https://doi.org/10.1109/MELECON53508.2022.9842895.
[68] R. Prater, T. Hanne, R. Dornberger, Generalized performance of LSTM in time-series forecasting, Appl. Artif. Intell. 38 (2024), https://doi.org/10.1080/08839514.2024.2377510/ASSET/CF45FB12-E584-477E-B839-88EE95A7B350/ASSETS/GRAPHIC/UAAI_A_2377510_F0003_B.GIF.
[69] G. Antonesi, T. Cioara, I. Anghel, I. Papias, V. Michalakopoulos, E. Sarmas, Hybrid transformer model with liquid neural networks and learnable encodings for buildings' energy forecasting, Energy and AI 20 (2025) 100489, https://doi.org/10.1016/J.EGYAI.2025.100489.
[70] F.M. Salem, R.N.N. Gated, The long short-term memory (LSTM) RNN, Recurrent Neural Network. (2022) 71–82, https://doi.org/10.1007/978-3-030-89929-5_4.
[71] X. Xu, L. Xia, Q. Zhang, S. Wu, M. Wu, H. Liu, The ability of different imputation methods for missing values in mental measurement questionnaires, BMC Med. Res. Methodol. 20 (2020) 1–9, https://doi.org/10.1186/S12874-020-00932-0/TABLES/3.
[72] Y. Jeong, E. Yang, J.H. Ryu, I. Park, M. Kang, AnomalyBERT: self-supervised transformer for time series anomaly detection using data degradation scheme, ArXiv Preprint (2023).
[73] A.J. Saroj, A. Guin, M. Hunter, Deep LSTM recurrent neural networks for arterial traffic volume data imputation, J. Big Data Analytics Transport. 3 (2021), https://doi.org/10.1007/s42421-021-00043-2.
[74] N.S. Dasappa, G.K. Kumar, N. Somu, Multi-sensor data fusion framework for energy optimization in smart homes, Renew. Sustain. Energy Rev. 193 (2024) 114235, https://doi.org/10.1016/J.RSER.2023.114235.
[75] S. Bourhnane, M.R. Abid, R. Lghoul, K. Zine-Dine, N. Elkamoun, D. Benhaddou, Machine learning for energy consumption prediction and scheduling in smart buildings, SN Appl. Sci. 2 (2020) 1–10, https://doi.org/10.1007/S42452-020-2024-9/FIGURES/11.
[76] N.M. Quy, L.A. Ngoc, N.T. Ban, N Van Hau, V.K. Quy, Edge computing for real-time internet of things applications: future internet revolution, Wirel. Pers. Commun. 132 (2023) 1423–1452, https://doi.org/10.1007/S11277-023-10669-W/FIGURES/2.
[77] B. Falcão, A. Annuk, M. Marinho, Employing machine learning for advanced gap imputation in solar power generation databases. https://doi.org/10.1038/s41598-024-74342-3, 2024.
[78] R. Gomila, C.S. Clark, Missing data in experiments: challenges and solutions, Psychol. Methods 27 (2022) 143–155, https://doi.org/10.1037/met0000361.
[79] R.C. Pereira, P.H. Abreu, P.P. Rodrigues, M.A.T. Figueiredo, Imputation of data missing not at random: artificial generation and benchmark analysis, Expert Syst. Appl. 249 (2024), https://doi.org/10.1016/j.eswa.2024.123654.